J. Biochem. 129, 917–922 (2001)

Structural and Functional Changes in Bovine Pancreatic Ribonuclease A by the Replacement of Phe120 with Other Hydrophobic Residues[1]

Eri Chatani, Naoki Tanimizu, Hiroshi Ueno, and Rikimaru Hayashi[2]

Division of Applied Life Sciences, Graduate School of Agriculture, Kyoto University, Sakyo-ku, Kyoto 606-8502

Received February 26, 2001; accepted March 22, 2001

To clarify the specific role of Phe120 in bovine pancreatic ribonuclease A (RNase A), changes in the thermal stability and activity of F120L, F120A, F120G, and F120W were analyzed with respect to some thermodynamic terms, *i.e.*, Gibbs free energy, enthalpy, and entropy. The structural destabilization of F120L, F120A, and F120G was due to a decrease in ΔH_m with a parallel decrease in amino-acid volume at position 120, while the destabilization of F120W can be ascribed to an increase in ΔS_m accompanying an increase in ΔH_m, showing that the size of Phe120 produces an optimum balance of conformational enthalpy and entropy for achieving the maximal structural stability. Moreover, the replacement of Phe120 affects activity. The increase in K_m showed that the hydrophobicity and π electron of Phe120 are important factors in substrate binding. The decrease in k_{cat} was predicted to be due to positional changes of the side chains of His12 and/or His119. The positional changes were successfully detected by the rate of carboxymethylation by iodoacetate or bromoacetate, which correlated very well with decreases in activity, supporting the view that Phe120 also plays an important role in determining the position of His12 and/or His119 in order to achieve efficient catalysis.

Key words: carboxymethylation rate, hydrophobicity, phenylalanine, π electron, RNase A.

Bovine pancreatic ribonuclease A (RNase A) [EC 3.1.27.5] is an endonuclease that cleaves at the 3′-end of pyrimidine nucleosides. Two histidine residues, His12 and His119, function in the catalysis as an acid and a base in an in-line mechanism, and Lys41 stabilizes the transition state (*1–3*). Six substrate binding subsites, P0, P1, P2, B1, B2, and B3, have been identified thus far and participate in substrate binding, *i.e.*, Lys66 at P0, Gln11, Phe120, and Asp121 at P1, Lys7 and Arg10 at P2, Thr45, Asp83, and Phe120 at B1, Asn71 and Glu111 at B2 (*2, 3*). Other amino acid residues also assist the catalytic residues: Asn121 maintains the proper tautomeric form of His119 *via* hydrogen bonding (*4–6*), and two disulfide bonds, Cys40–Cys95 and Cys65–Cys72, are important for retaining catalytic activity (*7*). Three residues located at the substrate binding site, Lys7, Arg10, and Lys66, influence the pK_a values of His12 and His119 for optimum catalysis (*8, 9*).

Phe120 is located in the vicinity of His12 and His119, and contributes to substrate binding at the P1 and B1 subsites (*10–13*). A previous study showed that not only K_m but also k_{cat} were affected as the result of the mutagenic replacement of Phe120 by other amino acid residues. This result indicates that Phe120 also contributes to catalysis (*13*). It is predicted that Phe120 may be important for maintaining the effective catalytic residues (*13*).

In this paper, in order to clarify the specific role of Phe120, F120G as well as F120L, F120A, and F120W mutant RNase A (see Ref. *13*) were newly prepared by the mutagenic replacement of Phe120, and their activities, thermal stabilities, and changes in the pK_a of His12 and His119 were compared with those of the wild-type enzyme by introducing energetic terms. As a strategy for evaluating the positional change of His12 and His119 caused by the mutagenic replacement of Phe120, carboxymethylation of the wild-type and mutant RNase A by bromoacetate or iodoacetate has also been examined: the carboxymethylation of RNase A occurs only at either His12 or His119 at pH 5.5–6.0, producing 1-CM-His-119RNase A and 3-CM-His-12RNase A (*14, 15*) in a unique yield ratio (*16–21*). The carboxymethylation requires the strict orientation of the alkylating reagent at the active site and it would be expected that even small changes in the active site of RNase A would be reflected in the rate of carboxymethylation (*18, 19, 21–24*).

MATERIALS AND METHODS

Materials—A DNA fragment coding the RNase A sequence was amplified from plasmid pSJII165, which was kindly provided by Prof. H.A. Scheraga of Cornell University, New York, USA. Using this DNA fragment, a plasmid for the expression of RNase A was constructed according to

[1] This work was supported, in part, by a Grant-in-Aid for Scientific Research from the Ministry of Education, Science, Sports and Culture of Japan, and a Grant from the Japan Society for the Promotion of Science (JSPS) for E.C.

[2] To whom correspondence should be addressed. Tel: +81-75-753-6110, Fax: +81-75-753-6128

Abbreviations: CpA, cytidinyl-3′,5′-adenosine; C>p, cytidine-2′,3′-cyclic monophosphate; IPTG, isopropyl-1-thio-β-D-galactoside.

the method of delCardayre *et al.* with minor modifications (*25, 26*). *Escherichia coli* strain BL21(DE3) [F^- *ompT* $hsdS_B$ (r_B-m_B-) *gal dcm* (DE3)] was obtained from Novagen (Milwaukee, USA). Oligonucleotides were synthesized by Japan Bioservice (Saitama). The Quickchange Site-Directed Mutagenesis Kit was obtained from Stratagene Cloning Systems (California, USA). The ABI Prism Big Dye™ Terminator Cycle Sequencing Ready Reaction DNA Sequencing Kit was purchased from Perkin Elmer (California, USA). IPTG and DTT, which were used in the *E. coli* expression system, were obtained from Nacalai Tesque (Kyoto). Commercial RNase A from Sigma (Type I-A, Missouri, USA), used as a control, was further purified by an FPLC apparatus equipped with a Mono S HR 5/5 column from Pharmacia (New Jersey, USA). A BCA assay kit was purchased from Pierce (Illinois, USA). Iodoacetate and bromoacetate were purchased from Nacalai Tesque and further purified by distillation under reduced pressure. CpA and C>p were purchased from Tokyo Kagaku Kogyo (Tokyo) and Nacalai Tesque, respectively.

Mutagenesis—Mutant plasmids for the expression of Phe120 mutant RNase A, F120A, F120G, and F120W were constructed with a Quickchange Site-Directed Mutagenesis Kit (Stratagene Cloning Systems). The sequences of the primers designated to replace the Phe120 codon with other amino acid codons were 5′-C GTT CCT GTC CAC TTG (for Leu)/GCT (for Ala)/GGT (for Gly)/TGG (for Trp) GAC GCC AGT GTT T-3′ and 5′-A AAC ACT GGC GTC CAA (for Leu)/AGC (for Ala)/ACC (for Gly)/CCA (for Trp) GTG GAC AGG AAC G-3′. The mutations introduced into the plasmid were confirmed by DNA sequencing using an ABI Prism Applied Biosystems 310 Genetic Analyzer (Perkin Elmer) by the dideoxy terminator sequencing method, and each mutated plasmid was introduced into BL21(DE3) strain cells. Transformed cells were selected by ampicillin resistance.

Production and Purification of Wild-Type and Mutant RNase A—Proteins were expressed by the method of Dodge and Scheraga (*26*) with the following minor modifications: the transformed strain was incubated in 1 liter of LB medium (1% tryptone, 0.5% yeast extract, and 1% NaCl, adjusted pH to 7.0) containing 50 μg/ml ampicillin at 37°C. Protein expression was induced by the addition of IPTG (final concentration 1 μM) after the cells were grown to an absorbance at 570 nm of 0.8, and then incubated for 3 h. The cells were harvested by centrifugation and suspended in 20 ml of 100 mM NaCl for sonication. The disrupted cells were centrifuged, resuspended in 12 ml of solubilization solution (20 mM Tris-HCl, pH 8.0, containing 7 M guanidine hydrochloride and 10 mM EDTA), and then stirred for 2–3 h. DTT was added to the solution to a final concentration of 0.1 M, and the solution was stirred for 30 min to solubilize proteins, including RNase A. After the addition of 108 ml of 20 mM acetic acid, the insoluble particles were removed by centrifugation, and the supernatant was dialyzed against 20 mM acetic acid. The solution was then mixed with 500 ml of refolding buffer (100 mM Tris-HOAc, pH 7.8, containing 0.1 M NaCl, 3.0 mM GSH, and 0.6 mM GSSG), stirred for 48 h at 4°C, and the pH of the solution was then lowered by adding 5 ml acetic acid in order to terminate the refolding reaction. The solution containing regenerated RNase A was concentrated using a Pellicon™-2 ultrafiltration system from Millipore (Massachusetts, USA) in conjunction with a 3,000 M_r cutoff membrane for purification.

The recombinant RNase A was purified by an FPLC apparatus (Pharmacia) equipped with a Mono S HR 5/5 column (7 × 54 mm, Pharmacia) equilibrated with 25 mM potassium phosphate buffer, pH 6.5. Elution was carried out with a linear gradient of 0.1 M NaCl/1.0 ml in the same buffer, at a flow rate of 1.0 ml/min. The purified enzyme was diluted 1,000-fold with water and concentrated using a Centricon (Millipore).

Protein Concentration—Protein concentration was determined by BCA assay (*27*) after each purification step. The standard curve for the assay was prepared using commercial RNase A.

CD Spectroscopy—CD spectra from 190 to 260 nm were measured on a Jasco J720 spectropolarimeter by the method described previously (*13*). The protein concentration was 10 μM in 10 mM MES buffer, pH 6.0.

Thermal Denaturation—Thermal denaturation was monitored by changes in the [θ] value at 222 nm by method similar to that described previously (*13*). The protein concentration was 5.0 μM in 10 mM MES buffer containing 0.1 M KCl, pH 6.0.

Fractions of native (f_N) and denatured enzymes (f_D), and the equilibrium constant for enzyme denaturation (K), were calculated according to Eqs. 1 to 3:

$$f_N = ([\theta]_D - [\theta])/([\theta]_D - [\theta]_N) \quad (1)$$

$$f_D = 1 - f_N \quad (2)$$

$$K = f_D/f_N \quad (3)$$

where [θ] represents the θ value at 222 nm of the sample, and $[\theta]_N$ and $[\theta]_D$ the [θ] of native and thermally-denatured enzymes at 222 nm, respectively.

The enthalpy at T_m (ΔH_m) was calculated according to the van't Hoff equation (4):

$$d(\ln K)/d(1/T) = -\Delta H_m/R \quad (4)$$

T_m is defined as the temperature when $K = 1$.

The entropy at T_m (ΔS_m) was calculated according to Eq. 5:

$$\Delta H_m - T_m \Delta S_m = 0 \quad (5)$$

Steady-State Kinetics—Transphosphorylation and hydrolysis activity were measured according to the method described previously (*13*). Transphosphorylation activity was assayed using 3–15 mM CpA as the substrate in 0.2 M sodium acetate buffer, pH 5.5, sodium phosphate buffer, pH 3.0. The hydrolytic activity was assayed using 1–10 mM C>p (*28*) in 0.2 M sodium acetate buffer, pH 5.5, at 25°C.

The values of k_{cat} and K_m were calculated from a Hanes-Woolf plot (*29*), based upon the model $E + S \rightleftarrows ES \rightarrow ES^{\ddagger} \rightarrow E + P$, in which $1/K_m$ represents an approximation of the equilibrium constant in $E + S \rightleftarrows ES$, since the process $ES \rightarrow ES^{\ddagger}$ is rate-limiting (*8*). Free energy changes in the processes $E + S \rightleftarrows ES$ ($\Delta\Delta G$) and $ES \rightarrow ES^{\ddagger}$ ($\Delta\Delta G^{\ddagger}$) were calculated according to Eqs. 6 and 7:

$$\Delta\Delta G = -RT \ln (K_m^{wt}/K_m^{mutant}) \quad (6)$$

$$\Delta\Delta G^{\ddagger} = -RT \ln (k_{cat}^{mutant}/k_{cat}^{wt}) \quad (7)$$

pH Dependence of Hydrolytic Activity—The hydrolysis reaction was measured at a substrate concentration of 1/5 the K_m values, and 200 mM NaCl in 20 mM buffer as described previously (*13*). The extinction coefficients of C>p and 3′-CMP at various pH values were determined experimentally and used in calculating the reaction rate. The k_{cat}/

K_m values were estimated according to Eq. 8, and the ln (k_{cat}/K_m) was plotted against pH.

$$v = (k_{cat}/K_m)\,[E]\,[S] \quad (8)$$

Inhibition by Phosphate Anions—The inhibition of hydrolytic activity by phosphate anion was measured in 200 mM sodium acetate buffer, pH 5.5, containing 0.073–8.5 μM enzyme and sodium phosphate concentrations in the range of 0–9 mM, adjusted to pH 5.5.

Carboxymethylation—Solutions containing 219 μM enzymes were reacted with 16 mM haloacetate in 10 mM sodium acetate buffer, pH 5.5, at 25.0°C in the dark as previously described (*17*). A portion of the reaction mixture was removed at various times for the determination of the hydrolytic activity. Reaction kinetics were analyzed as the second-order reactions using Eqs. 9 and 10:

$$dx/dt = -k_{CM}([E_0]-x)([I_0]-x) \quad (9)$$

$$1/([E_0]-[I_0])\ \ln\{[[I_0]([E_0]-x)]/[[E_0]([I_0]-x)]\} = -k_{CM}t \quad (10)$$

where k_{CM} is the second order rate constant for the carboxymethylation reaction, x the concentration of enzyme that reacted with haloacetate, and $[E_0]$ and $[I_0]$ the initial concentrations of enzyme and haloacetate, respectively.

Two carboxymethylated derivatives, 1-CMHis119-RNase A and 3-CMHis12-RNase A, were separated on a Mono S HR 5/5 column (Pharmacia) equilibrated with 25 mM potassium phosphate buffer, pH 7.5. Protein was eluted with a linear gradient with a 10% increase in 0.5 M potassium phosphate buffer, pH 7.5, per 15 min at a flow rate of 1.0 ml/min. The ratio of the yield of the derivatives was determined by integrating the areas corresponding to the individual elution peaks. The carboxymethyla-tion rate constants of His12 ($k_{CM\text{-}His12}$) and His119 ($k_{CM\text{-}His119}$) were calculated by multiplying the overall rate constant, k_{CM}, and their ratio of their yields.

Gibbs energies of the carboxymethylations at His12 and His119 [$(\Delta\Delta G+\Delta\Delta G^{\ddagger})_{CM\text{-}His12}$ and $(\Delta\Delta G+\Delta\Delta G^{\ddagger})_{CM\text{-}His119}$, respectively] were calculated according to Eqs. 11 and 12:

$$(\Delta\Delta G+\Delta\Delta G^{\ddagger})_{CM\text{-}His12} = -RT\ln(k_{CM\text{-}His12}{}^{mutant}/k_{CM\text{-}His12}{}^{wt}) \quad (11)$$

$$(\Delta\Delta G+\Delta\Delta G^{\ddagger})_{CM\text{-}His119} = -RT\ln(k_{CM\text{-}His119}{}^{mutant}/k_{CM\text{-}His119}{}^{wt}) \quad (12)$$

RESULTS

Expression and Purification of Mutant RNase A—Approximately 4.5 g (wet weight) of *E. coli* pellet was obtained from 1 liter of culture medium of wild type and mutant RNase A (F120L, F120A, F120G, and F120W). All of the purified enzymes gave single bands on SDS-PAGE after the final purification step in final yields of approximately 20 mg. The molecular masses of the wild type and mutant enzymes measured by MALDI-TOF mass spectrometry (Voyager RP, PerSeptive Biosystems, California, USA) were in good agreement with the theoretical molecular masses, indicating success in obtaining the expected mutants.

Structural Changes by Mutation of Phe120—The CD spectra of F120G, F120L, F120A, and F120W and wild-type RNase A were nearly identical, as shown in the previous report (*13*), suggesting that mutations at Phe120 cause no substantive change in the secondary structure.

The thermal denaturation of the wild-type and all mutant enzymes was completely reversible and consistent with the theoretical two-state transition curve (Fig. 1). Energetic parameters and T_m values for thermal denaturation are summarized in Table I. $\Delta G_{59.7°C}$ (59.7°C is T_m of wild-type RNase A) and T_m decreased in the order of wild-type RNase A > F120L > F120W > F120A > F120G. ΔH_m decreased in the order of F120W > wild-type RNase A > F120L > F120A > F120G. The decrease in ΔH_m shows linearity with the decrease in the volume change of the substituted amino acid residues. This indicates that the van der Waals volume of the side chain is important for bonding at position 120. It is reasonable to think that the thermal destabilization of F120L, F120A, and F120G mutant RNase A is due to the loss of bonding energy at position 120. On the other hand, the thermal destabilization of F120W is lower than that of the wild-type enzyme, despite its larger ΔH_m value. We conclude that this destabilization is due to an increase in ΔS_m; an increase in structural rigidity of the protein that is accompanied by an increase in ΔH_m, thus causing the destabilization.

Activity Change Caused by the Mutation of Phe120—Energetic parameters, $\Delta\Delta G$, and $\Delta\Delta G^{\ddagger}$ of the wild-type– and

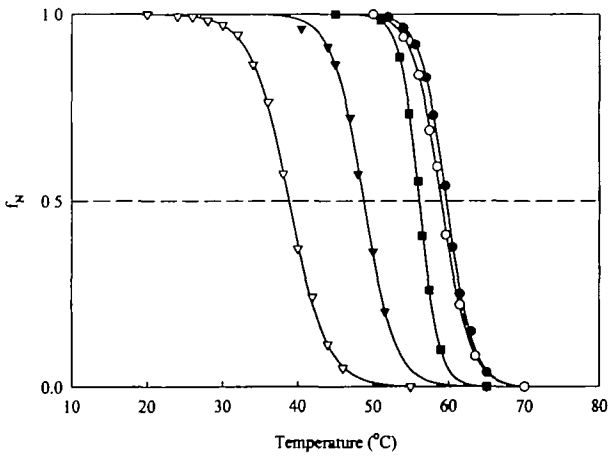

Fig. 1. **Thermal denaturation of the wild type (closed circles) and F120G (open triangles) RNase A.** The data for F120L (open circles), F120A (closed triangles), and F120W (closed squares) were taken from Ref. *13*. Solid lines represent the theoretical sigmoidal curves for a two-state transition, all of which were found to fit very well with the observed plots. T_m and energetic parameters ($\Delta G_{59.7°C}$, ΔH_m, and ΔS_m) were calculated from these sigmoidal curves (see Table I).

TABLE I. **Thermal stability of wild-type and mutant RNase A.**

Enzyme	ΔH_m (kJ mol^{-1})	ΔS_m (kJ mol^{-1} K^{-1})	T_m (°C)	$\Delta G_{59.7°C}$ (kJ mol^{-1})	van der Waals volume of the amino acid residue at 120 (Å^3)
Wild type	548.8 ± 9.7	1.65 ± 0.04	59.7	0	135
F120L	491.9 ± 7.0	1.48 ± 0.02	59.0	−1.03 ± 0.05	124
F120A	418.8 ± 8.6	1.30 ± 0.03	48.9	−14.1 ± 0.3	67
F120G	301.2 ± 7.6	0.97 ± 0.02	38.8	−20.2 ± 0.6	48
F120W	706.9 ± 10.3	2.15 ± 0.03	56.2	−7.54 ± 0.13	163

mutant enzyme–catalyzed transphosphorylation and hydrolytic reactions were calculated from K_m and k_{cat}, respectively, and are summarized in Table II.

$\Delta\Delta G$ for the mutant RNase A increased linearly as the hydrophobicity (*30*) of the amino acid residue at position 120 decreased in the order of F120L > F120W > F120A > F120G. However, only $\Delta\Delta G$ of the wild-type RNase A was much greater than $\Delta\Delta G$, which would be expected only from the hydrophobicity, probably due to π electrons that participate in substrate binding at the B1 substrate binding subsite.

The K_i values of phosphate for the wild-type and all mutant enzymes were similar, suggesting that the P1 subsite is insignificantly altered by mutation of Phe120.

$\Delta\Delta G^{\ddagger}$ of F120L was very small, implying that the transition states for the wild-type and F120L enzymes are similar; but $\Delta\Delta G^{\ddagger}$ of F120A, F120G, and F120W are clearly larger than the $\Delta\Delta G^{\ddagger}$ of the wild-type enzyme, with respect to both the transphosphorylation and hydrolytic activities. This indicates that not only substrate binding but also catalytic rate is affected by the mutation of Phe120. Since there are no interrelationships among $\Delta\Delta G^{\ddagger}$ values, volume, and hydrophobicity of the substituted amino acid residues, the residue at position 120 may not participate directly in the catalytic reaction.

pK_a Changes in His12 and His119 as a Result of the Mutation of Phe120—The pK_a of His12 and His119 in F120G, as calculated from the pH curve (*31*), were the same as those for F120L, F120A, and F120W RNase A, which were determined as previously reported (*13*). This result indicates that the significant changes in k_{cat}/K_m (Table II) are probably due to positional changes in His12 and/or His119, which may be caused by the mutation of Phe120.

Carboxymethylation at His12 or His119—When the left side of Eq. 10 is plotted against time, a straight line is obtained for wild-type and mutant enzymes with a correlation coefficient >0.99, giving an over-all second order constant, k_{CM}. The reaction mixture yielded three peaks (Fig. 2). The middle peak, which decreased with reaction time, was identified as unmodified RNase A, and the peaks that eluted before and after the unmodified RNase A were identified as 1-CMHis-119-RNase A and 3-CMHis-12-RNase A, respectively, by Maldi-Tof mass spectrometry. The ratio of the two peak areas was 85:15 in the case of wild-type enzyme reacted with iodoacetate (Table II). Although the elution profile was different from the previous result in which an IRC-50:NaCl system was used (*15–17*), the ratio is in agreement with the reported ratio of 1-CMHis-119-RNase A and 3-CMHis-12-RNase A, respectively (*17*).

The carboxymethylation of RNase A has been explained by the Michaelis-Menten equation (*18, 21*), where k_{CM} is regarded to be k_{catCM}/K_{mCM} of the overall carboxymethylation (K_m and k_{cat} represent the equilibration constant for the binding of haloacetate to RNase A and the rate constant for carboxymethylation, respectively). Therefore, k_{catCM}/K_{mCM} for the carboxymethylation of His12 and His119 can be approximated to $k_{CM\text{-}His12}$ and $k_{CM\text{-}His119}$, respectively. $(\Delta\Delta G+\Delta\Delta G^{\ddagger})_{CM\text{-}His12}$ and $(\Delta\Delta G+\Delta\Delta G^{\ddagger})_{CM\text{-}His119}$, which were calculated from $k_{CM\text{-}His12}$ and $k_{CM\text{-}His119}$, are given in Table III.

The reactivities of iodoacetate and bromoacetate were similar for the wild-type and all mutant RNase A samples as follows: $(\Delta\Delta G+\Delta\Delta G^{\ddagger})_{CM\text{-}His119}$ of F120L RNase A was nearly zero, whereas those of F120A, F120G, and F120W showed

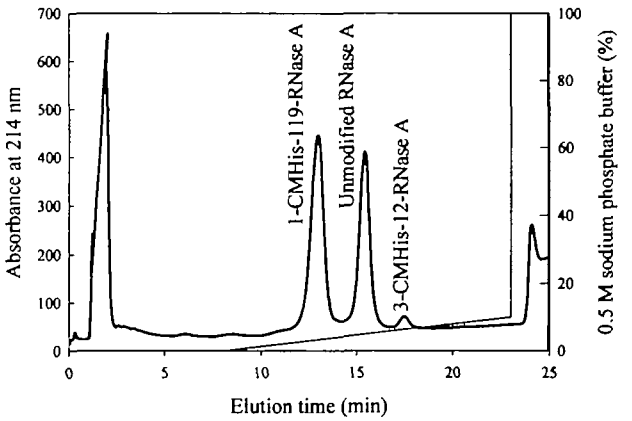

Fig. 2. **Chromatographic separation of 1-CMHis-119-RNase A, 3-CMHis-12-RNase A, and unmodified RNase A after the reaction of wild-type RNase A with iodoacetate.** A MonoS HR 5/5 column equilibrated with 25 mM potassium phosphate buffer, pH 7.5, was used for the separation. Thick and thin solid lines represent the absorbance at 214 nm and the 0.5 M sodium phosphate buffer gradient, respectively.

TABLE II. **Kinetic and energetic parameters for CpA and C>p, and the K_i values for phosphate in wild-type and mutant RNase A.**

Enzyme	CpA					C>p						Hydrophobicity of side chain at 120[d] (kJ mol^{-1})
	k_{cat}[c] (s^{-1})	K_m[c] (mM)	k_{cat}/K_m (mM^{-1} s^{-1})	$\Delta\Delta G^{\ddagger}$[a] (kJ mol^{-1})	$\Delta\Delta G^{\ddagger}$[a] (kJ mol^{-1})	k_{cat}[c] (s^{-1})	K_m[c] (mM)	k_{cat}/K_m (mM^{-1} s^{-1})	$\Delta\Delta G^{\ddagger}$[a] (kJ mol^{-1})	$\Delta\Delta G^{\ddagger}$[a] (kJ mol^{-1})	K_i[b] (mM)	
Wild type	1,800 ±100	0.67 ±0.05	2,700 ±200	0	0	2.7±0.2	0.62 ±0.06	4.2±0.3	0	0	6.4 ±0.8	−8.57
F120L	2,800 ±200	3.5 ±0.4	800 ±30	4.1±0.3	−1.1 +0.2	1.8±0.2	1.7 ±0.1	1.1±0.1	2.5±0.4	1.0±0.5	10 ±2	−16.71
F120A	1,300 ±200	13 ±3	96 ±10	7.3±0.6	0.8±0.4	0.62 ±0.03	7.9 ±0.4	0.078 ±0.01	6.3±0.4	3.6±0.3	10 ±1	−3.65
F120G	120 ±4	22 ±3	5.4 ±0.7	8.7±0.3	6.7±0.1	0.39 ±0.02	13 ±1	0.025 ±0.000	7.7±0.6	4.9±0.4	5.5 ±1.4	0
F120W	470 ±60	7.3 ±0.9	64 ±2	5.9±0.3	3.3±0.4	0.23 ±0.02	4.0 ±0.2	0.058 ±0.003	4.6±0.4	6.1±0.4	11 ±1	−5.84

[a] $\Delta\Delta G$ and $\Delta\Delta G^{\ddagger}$ equal to $(\Delta G_{mutant\ enzyme}-\Delta G_{wild\text{-}type})$ and $(\Delta G^{\ddagger}_{mutant\ enzyme}-\Delta G^{\ddagger}_{wild\text{-}type})$, respectively. [b] K_i is the parameter for the inhibitory effect by phosphate anion relative to the hydrolytic activity of C>p. [c] k_{cat}, K_m and for wild-type, F120L, F120A, and F120W were taken from our previous paper (Ref. *13*). [d] Side chain hydrophobicity data were taken from Ref. *30*.

TABLE III. **Carboxymethylation of wild-type and mutant RNase A by reaction with bromoacetate and iodoacetate.**

Reagent	Enzyme	k_{CM} ($\times 10^{-4}$ mol^{-1} s^{-1})	Product ratio	$k_{CM\text{-}His119}$* ($\times 10^{-4}$ mol^{-1} s^{-1})	$k_{CM\text{-}His12}$* ($\times 10^{-4}$ mol^{-1} s^{-1})	$(\Delta\Delta G+\Delta\Delta G^{\ddagger})_{CM\text{-}His119}$ (kJ mol^{-1})	$(\Delta\Delta G+\Delta\Delta G^{\ddagger})_{CM\text{-}His12}$ (kJ mol^{-1})
Bromoacetate	Wild type	279.0 ± 11.9	95: 5	265.1 ± 11.3	14.0 ± 0.6	0	0
	F120L	277.7 ± 0.0	93: 7	263.8 ± 0.0	13.0 ± 0.0	0.019 ± 0.097	0.18 ± 0.11
	F120A	100.6 ± 15.1	76:24	76.5 ± 11.5	24.1 ± 3.6	3.1 ± 0.5	−1.4 ± 0.7
	F120G	113.0 ± 40.0	97: 3	109.6 ± 38.8	3.4 ± 1.2	2.2 ± 1.2	3.5 ± 1.2
	F120W	90.9 ± 0.0	78:22	70.9 ± 0.0	20.0 ± 0.0	3.3 ± 0.1	−0.88 ± 0.10
Iodoacetate	Wild type	114.8 ± 17.9	85:15	97.6 ± 15.2	17.2 ± 2.7	0	0
	F120L	88.4 ± 7.9	90:10	79.6 ± 7.1	6.8 ± 1.2	0.51 ± 0.59	2.3 ± 0.8
	F120A	33.7 ± 0.3	76:24	25.8 ± 0.2	8.1 ± 0.1	3.3 ± 0.4	1.9 ± 0.4
	F120G	28.9 ± 0.0	96: 4	27.7 ± 0.0	1.2 ± 0.0	3.1 ± 0.4	6.6 ± 0.4
	F120W	20.1 ± 0.1	72:28	14.5 ± 0.1	5.6 ± 0.0	4.7 ± 0.4	2.8 ± 0.3

*$k_{CM\text{-}His119}$ and $k_{CM\text{-}His12}$ were calculated by multiplying $k_{overall}$ and the product ratio for yields.

significant values. On the other hand, $(\Delta\Delta G+\Delta\Delta G^{\ddagger})_{CM\text{-}His12}$ for F120A, F120G, and F120W were found to have significant values. In particular, that of F120G RNase A was the highest. The total of $(\Delta\Delta G+\Delta\Delta G^{\ddagger})_{CM\text{-}His119}$ and $(\Delta\Delta G+\Delta\Delta G^{\ddagger})_{CM\text{-}His12}$ were in the order of F120L > F120A > F120W > F120G, which is in agreement with the order of k_{cat}.

DISCUSSION

Role of Phe120 in Conformational Stability—The proportional relationship between bonding energy (ΔH_m) and the volume of amino acid residue 120 (see Table I) shows the importance of the volume of Phe120 in terms of thermal stability. However, overly strong bondings destabilize the conformation, as can be seen in the case of F120W RNase A, since an increase in bonding energy at residue 120 is accompanied by a loss of conformational freedom. Interestingly, the presence of Phe120 provides for an exquisite balance between conformational enthalpy and entropy, giving rise to the most stable conformation of RNase A.

Role of Phe120 in Substrate Binding—The lack of any significant change in the K_i values of the mutant enzymes indicates only a small change in the P1 subsite. Thus, an increase in K_m values following the replacement of Phe120 with leucine, glycine, alanine, or tryptophan (see Table II) suggests that the side chain of Phe120 is important at the B1 subsite (*12*): the increase in K_m in the case of the mutant enzymes can be attributed to the weakened affinity of the side chain at position 120 to the pyrimidine base. The decreased binding affinity of F120L, which has a larger hydrophobicity (*30*) (Table II) but no π electron, is consistent with the previous crystallographic results of an RNase A and 3′-CMP or d(CpA) complex, in which the benzene ring of Phe120 binds to the pyrimidine base of the substrate *via* π-electron stacking (*12*). The substrate affinity at the B1 subsite also decreases with decreasing hydrophobicity of the amino acid residue at position 120 (Table II), showing that hydrophobic interactions between Phe120 and the substrate are not negligible, as has been previously reported (*31*).

The replacement of the substrate binding residue in general can lead to a change in the substrate binding mode, but this possibility can be ruled out in the present case of Phe120 mutant enzymes because the $\Delta\Delta G$ values for the mutant enzymes are very similar to one another in terms of both the transphosphorylation and hydrolytic reactions [the difference in $\Delta\Delta G$ for the two reactions was only 1.0 ± 0.2 kJ mol^{-1} for all mutants (Table II)]. It can be concluded that Phe120 is an important contributor to substrate affinity.

The substrate affinity of F120W is higher than that of F120G and F120A, and lower than that of F120L, even though Trp120 has π electrons and hydrophobicity similar to Phe120 (*30*). This result indicates that the large volume of the tryptophan residue prevents the interaction with substrate.

Role of Phe120 in Catalysis—Substitution of Phe120 to leucine resulted in no change in k_{cat}, indicating that the π electrons of Phe120 make no direct contribution to stabilizing the transition state. Since the substrate binding mode in all mutant enzymes appeared to be similar to that of the wild-type RNase A as described above, the higher $\Delta G^{\ddagger}$ value for F120A, F120G, and F120W compared with the wild-type RNase A can be accounted for by the change in catalytic residues. Since the pK_a at His12 and His119 showed no change in the case of wild-type or mutant RNase A (*13*), it can be concluded that the change in k_{cat} in the mutant enzymes is restricted to positional changes of His12 and/or His119.

The carboxymethylation rate was sensitive to mutations at Phe120, as expected. The results of carboxymethylation indicate that either His12 or His119, or possibly both, change position as a result of the mutation of Phe120. The good correlation of the total carboxymethylation change, $(\Delta\Delta G+\Delta\Delta G^{\ddagger})_{CM\text{-}His12}+(\Delta\Delta G+\Delta\Delta G^{\ddagger})_{CM\text{-}His119}$, and activity (Table III) supports the conclusion that the decrease in k_{cat} is caused by positional changes in His12 and/or His119. That is, the correct spatial position of His12 and/or His119 is essential for RNase A activity. To estimate whether His12 and His119 move, or to what degree and how they change their positions as a result of Phe120 mutation, the details of the mechanisms of the carboxymethylation reaction of RNase A must be clarified.

What degree of positional change can occur at His12 and/or His119 in Phe120 mutant RNase A? According to the crystal structures of the F120L and F120Y mutants of semisynthetic RNase A (PDBcode: 1SSA and 1SSB, respectively) (*32*) and wild-type semisynthetic RNase A (PDBcode: 1SRN) (*33*), the distances between $N_{\delta 1}$ of His119 and $N_{\epsilon 2}$ of His12 in the wild type, F120Y and F120L enzymes are 7.27, 6.90, and 6.75 Å, respectively, showing a correlation with the decrease in activity. According to the crystal structures of D121N (PDBcode: 3RSD), D121A (PDBcode: 4RSD) (*6*), and wild-type RNase A (PDBcode: 1RPH) (*12*), the distance between the $N_{\delta 1}$ of His119 and the $N_{\epsilon 2}$ of His12 in the wild-type, D121N, and D121A enzymes are 6.38,

6.27, and 5.78 Å, respectively, also showing a correlation with the drastic decrease in activity. In these studies, D121N and D121A showed no change in the pK_a of His12 and His119 (*4–6*), similar to the results of the Phe120 mutants used in the present study. These studies suggest that small differences in the range of 1 Å may cause drastic decreases in activity.

CONCLUSION

Phe120 of bovine pancreatic RNase A, which is located close to His12 and His119 and is composed of a hydrophobic core, contributes to the maintenance of the optimum conformational stability and activity, playing the three following roles: (i) its optimum volume contributes to conformational stability; (ii) its π-electron interactions and hydrophobicity contribute to substrate binding; and (iii) it contributes to the correct maintenance of the spatial position of His12 and/or His119. The third role of Phe120 is possibly to be responsible for the very strict positioning of His12 and/or His119, based on comparisons of activity according to the distance between the $N_{\delta 1}$ of His119 and the $N_{\varepsilon 2}$ of His12 in the crystal structures of some mutant enzymes: deviations of these histidine residues within 1 Å, result in dramatic decreases in activity.

REFERENCES

1. Richards, F.M. and Wyckoff, H.W. (1971) Bovine pancreatic ribonuclease in *Enzymes* (Boyer, P.D., ed.) Vol. 4, pp. 722–734, Academic Press, New York
2. Raines, R.T. (1998) Ribonuclease A. *Chem. Rev.* **98**, 1045–1066
3. Cuchillo, C.M., Vilanova, M., and Nogues, M.V. (1997) Pancreatic ribonucleases in *Ribonucleases: Structures and Functions* (D'Alessio, G. and Riordan, J.F., eds.) pp. 271–300, Academic Press, New York
4. Quirk, D.J., Park, C., Thompson, J.E., and Raines, R.T. (1998) His...Asp catalytic dyad of ribonuclease A: Conformational stability of the wild-type, D121N, D121A, and H119A enzymes. *Biochemistry* **37**, 17958–17964
5. Quirk, D.J. and Raines, R.T. (1999) His...Asp catalytic dyad of ribonuclease A: histidine pK_a values in the wild-type, D121N, and D121A enzymes. *Biophys. J.* **76**, 1571–1579
6. Schultz, L.W., Quirk, D.J., and Raines, R.T. (1998) His...Asp catalytic dyad of ribonuclease A: Structure and function of the wild type, D121N, and D121A enzymes. *Biochemistry* **37**, 8886–8898
7. Klink, T.A., Woycechowsky, K.J., Taylor, K.M., and Raines, R.T. (2000) Contribution of disulfide bonds to the conformational stability and catalytic activity of ribonuclease A. *Eur. J. Biochem.* **267**, 566–572
8. Fisher, B.M., Ha, J.-H., and Raines, R.T. (1998) Coulombic forces in protein-RNA interactions: Binding and cleavage by ribonuclease A and variants at Lys7, Arg10, and Lys66. *Biochemistry* **37**, 12121–12132
9. Fisher, B.M., Schultz, L.W., and Raines, R.T. (1998) Coulombic effects on remote subsites on the active site of ribonuclease A. *Biochemistry* **37**, 17386–17401
10. Hayashi, R., Moore, S., and Merrifield, R.B. (1973) Preparation of pancreatic ribonuclease 1-114 and 1-115 and their reactivation by mixture with synthetic COOH-terminal peptides. *J. Biol. Chem.* **248**, 3889–3892
11. delCardayre, S.B. and Raines, R.T. (1994) Structural determinants of enzymatic processivity. *Biochemistry* **33**, 6031–6037
12. Zegers, I., Maes, D., Dao-thi, M., Poortmans, F., Palmer, R., and Wyns, L. (1994) The structures of RNase A complexed with 3'-CMP and d(CpA): Active site conformation and conserved water molecules. *Protein Sci.* **3**, 2322–2339
13. Tanimizu, N., Ueno, H., and Hayashi, R. (1998) Role of Phe120 in the activity and structure of bovine pancreatic ribonuclease A. *J. Biochem.* **124**, 410–416
14. Gundlach, H.G., Stein, W.H., and Moore, S. (1959) The nature of the amino acid residues involved in the inactivation of ribonuclease by iodoacetate. *J. Biol. Chem.* **234**, 1754–1760
15. Crestfield, A.M., Stein, W.H., and Moore, S. (1963) Alkylation and identification of the histidine residues at the active site of ribonuclease. *J. Biol. Chem.* **238**, 2413–2420
16. Crestfield, A.M., Stein, W.H., and Moore, S. (1963) Properties and conformation of the histidine residues at the active site of ribonuclease. *J. Biol. Chem.* **238**, 2421–2428
17. Heinrikson, R.L., Stein, W.H., Crestfield, A.M., and Moore, S. (1965) The reactivities of the histidine residues at the active site of ribonuclease toward halo acids of different structures. *J. Biol. Chem.* **240**, 2921–2934
18. Plapp, B.V. (1973) Mechanisms of carboxymethylation of bovine pancreatic nucleases by haloacetates and tosylglycolate. *J. Biol. Chem.* **248**, 4896–4900
19. Stark, G.R., Stein, W.H., and Moore, S. (1961) Relationships between conformation of ribonuclease and its reactivity toward iodoacetate. *J. Biol. Chem.* **236**, 436–442
20. Cederholm, M.T., Stuckey, J.A., Doscher, M.S., and Lee, L. (1991) Histidine pK_a shifts accompanying the inactivating Asp121-Asn substitution in a semisynthetic bovine pancreatic ribonuclease. *Proc. Natl. Acad. Sci. USA* **88**, 8116–8120
21. Lennette, E.P. and Plapp, B.V. (1979) Transition-state analysis of the facilitated alkylation of ribonuclease A by bromoacetate. *Biochemistry* **18**, 3938–3946
22. Lin, M.C. (1970) The structural roles of amino acid residues near the carboxyl terminus of bovine pancreatic ribonuclease A. *J. Biol. Chem.* **245**, 6726–6731
23. Lin, M.C., Stein, W.H., and Moore, S. (1968) Further studies on the alkylation of the histidine residues at the active site of pancreatic ribonuclease. *J. Biol. Chem.* **243**, 6167–6170
24. Gutte, B., Lin, M.C., Caldi, D.G., and Merrifield, R.B. (1972) Reactivation of des(119-, 120-, or 121-124) ribonuclease A by mixture with synthetic COOH-terminal peptide of varying length. *J. Biol. Chem.* **247**, 4763–4767
25. delCardayre, S.B., Ribo, M., Yokel, E.M., Quirk, D.J., Rutter, W.J., and Raines, R.T. (1995) Engineering ribonuclease A: production, purification and characterization of wild-type enzyme and mutant at Gln11. *Protein Eng.* **8**, 261–273
26. Dodge, R.W. and Scheraga, H.A. (1996) Folding and unfolding kinetics of the proline-to-alanine mutants of bovine pancreatic ribonuclease A. *Biochemistry* **35**, 1548–1559
27. Smith, P.K., Krohn, R.I., Hermanson, G.T., Mallia, A.K., Gartner, F.H., Provenzano, M.D., Fujimoto, E.K., Goeke, N.M., Olson, B.J., and Klenk, D.C. (1985) Measurement of protein using bicinchoninic acid. *Anal. Biochem.* **150**, 76–85
28. Moussaoui, M., Nogues, M.V., Guasch, A., Barman, T., Travers, F., and Cuchillo, C.M. (1998) The subsites structure of bovine pancreatic ribonuclease A accounts for the abnormal kinetic behavior with cytidine 2',3'-cyclic phosphate. *J. Biol. Chem.* **273**, 25565–25572
29. Cornish-Bowden, A. (1976) *Principles of Enzyme Kinetics*, p. 25, Butterworths, London
30. Radzicka, A. and Wolfenden, R. (1988) Comparing the polarities of the amino acids: side-chain distribution coefficients between the vapor phase, cyclohexane, 1-octanol, and neutral aqueous solution. *Biochemistry* **27**, 1664
31. Eftink, M.R. and Biltonen, R.L. (1983) Energetics of ribonuclease A catalysis. 1. pH, ionic strength, and solvent isotope dependence of the hyrolysis of cytidine cyclic 2',3'-phosphate. *Biochemistry* **22**, 5123–5134
32. de Mel, V.S.J., Docher, M.S., Glinn, M.A., Martin, P.D., Ram, M.L., and Edwards, B.F.P. (1994) Structural investigation of catalytically modified F120L and F120Y semisynthetic ribonucleases. *Protein Sci.* **3**, 39–50
33. Martin, P.D., Doscher, M.S., and Edwards, B.F.P. (1987) The refined crystal structure of semisynthetic ribonuclease at 1.8 Å resolution. *J. Biol. Chem.* **262**, 15930–15938